A High Affinity and Selective Recognition Element for Kynurenic Acid

Submitted by

Anna Francesca Karle

Biomedical Sciences

To

The Honors College

Oakland University

In partial fulfillment of the

requirement to graduate from

The Honors College

Mentor: Dr. Ngong Kodiah Beyeh, Assistant Professor of Chemistry

Department of Chemistry

Oakland University

1 April 2022

ABSTRACT

Kynurenic acid (KynA) is a byproduct of tryptophan (Trp) metabolism as well as an important neuroprotective biomolecule.[1–5] KynA acts as a distinct biomarker for many neurological diseases since concentrations above or below an established equilibrium are associated with clinically diagnosed schizophrenia and depression, respectively.[6–18] Currently, the only way to quantify KynA at physiological concentration levels is through high performance liquid chromatography (HPLC) analysis with extensive sample preparation.[19] This technique is also very expensive and time consuming.[20] A more efficient sensing system can achieve the same results utilizing a macrocyclic resorcin[4]arene receptor with inherent photophysical properties. This advancement is necessary as increasing amounts of research is associating KynA with depression, especially in women on oral contraceptives.[21–27] Having access to point of care testing for KynA blood levels can help guide physicians when diagnosing patients and prescribing medications. In this thesis research, a naphthalene functionalized resorcin[4]arene based receptor (Np-NAR(Cl)$_4$) displays high affinity and selectivity for KynA over Trp in a host-guest complex. The interactions are tested using Nuclear Magnetic Resonance (NMR) for qualitative screening, Isothermal Calorimetry (ITC) for quantitative thermodynamic parameters, Ultraviolet-Visible (UV-Vis) and Fluorescence Spectroscopy for visualizing binding across a range of pathological and physiological concentrations.

CHAPTER 1

1.0 INTRODUCTION

Supramolecular host-guest organic chemistry has been the interest of many research teams as point of care testing has become increasingly desirable in the medical field for quick test results.[28–30] The development of organic sensory recognition elements for a variety of clinically relevant biomolecules allows for the production of quantification blood assays.[31] Macrocycles act as hosts (or receptors) because they possess a hydrophobic interior cavity for guest binding (Figure 1-1). Each receptor has a core that is functionalized to match the environment its corresponding guest exists in. This means that receptors can be effective in multiple solvents and systems depending on their hand-picked design.[32] Some properties to consider when adding functional groups to an organic receptor core include (1) selectivity for a biomolecule over its precursors and (2) sensitivity for the biomolecule in its physiological as well as pathological concentrations. Another essential property to consider is the cost effectiveness of the hosts since the goal of production is to decrease the cost of clinical testing and increase the accessibility of tests to patients. In this thesis research, we explore the first report of a high affinity and selective macrocyclic receptor for KynA. We also report on the sensitivity, stability, and cost effectiveness of the receptor for potential applications in clinical research.

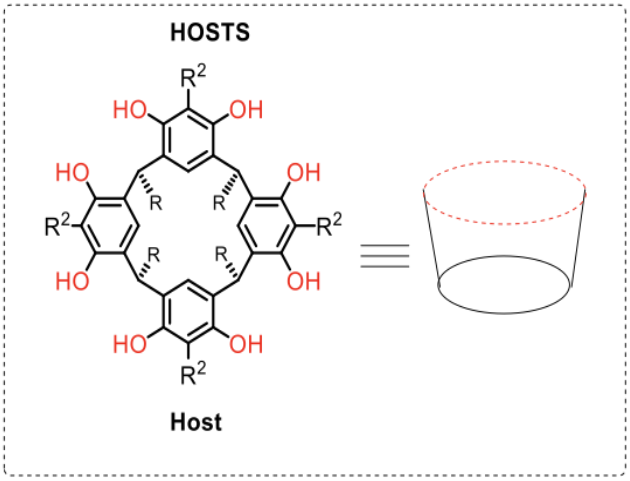

Figure 1-1: Resorcin[4]arene core showing internal hydrophobic cavity and a pictorial representation of the receptor in solution.

1.1 AIMS & OBJECTIVES

A naphthalene functionalized resorcin[4]arene macrocycle (Figure 1-2A) with high affinity and selectivity for KynA (Figure 1-2B) over its precursor Trp (Figure 1-2C) is reported in our most recent manuscript which is currently under peer-review in consideration for publication in the Analyst.[33] This thesis research augments the discovery of the host's sensing ability for KynA by discussing different practical properties that are necessary for a clinical biosensor. The following three objectives will be discussed:

(1) cost effectiveness for the synthesis of the Np-NAR(Cl)$_4$ host,

(2) sensitivity of the Np-NAR(Cl)$_4$ sensor for KynA in physiological and pathological concentrations, and

(3) stability of the KynA-host complex in solution over time.

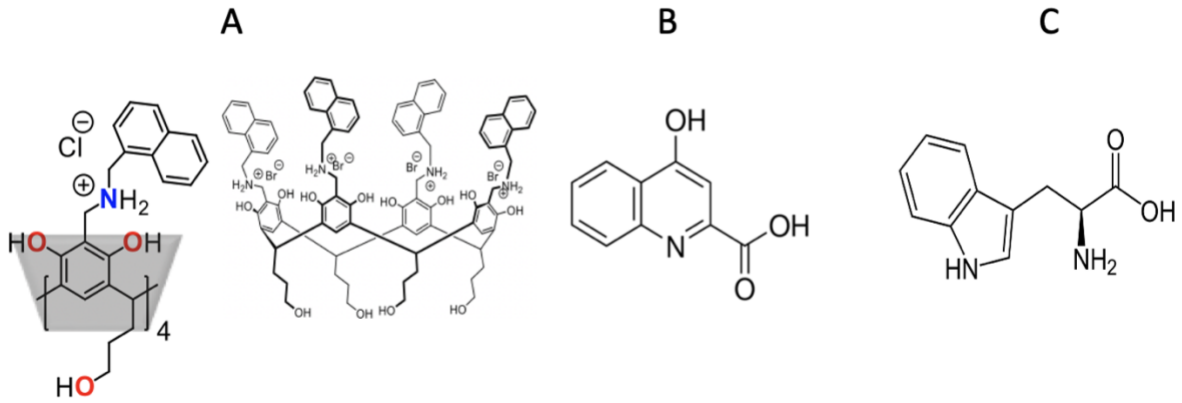

Figure 1-2: (A) Condensed and expanded forms of Np-NAR(Cl)$_4$, (B) Structure of KynA, (C) Structure of Trp

1.2 SIGNIFICANCE

Major depressive disorder is the leading cause of disability in America, affecting more than 16 million adults ages 15 to 44.[34–36] Relating depression specifically to women's health, postpartum depression affects 1 in 8 new mothers after childbirth.[37,38] Many women in America rely on oral contraceptives as their primary mechanism of family planning, however, there are intense side effects for some of these women that are often overlooked. Women who suffer from contraceptive-induced depression typically remain untreated as the phenomenon is not well understood by the medical community. This is because no research has reliably confirmed a causative relationship between depression and birth control even though some researchers have found correlations between the two.[39] Recent studies have provided a correlative relationship between KynA and depression, providing a physiological mechanism for birth control induced depression.[22] Low

KynA levels are commonly observed among oral contraceptive users and these low levels are, in turn, separately correlated to depression.[40–44]

A necessary component of this research is the ability to efficiently quantify physiological concentrations of KynA in a patient's blood plasma. As previously mentioned, HPLC analysis is the current technique used to quantify KynA concentrations in blood plasma, but has concerning pitfalls.[45] This technique requires extensive sample preparation, is time consuming, and expensive. Developing and optimizing an organic sensor molecule for research and clinical applications of physiological KynA quantifications increases the accessibility of future testing to screen patients for predispositions to drug-induced depression.

CHAPTER 2

2.0 SYNTHESIS AND FUNCTIONALIZATION OF RESORCIN[4]ARENE RECEPTOR

Synthesis of Np-NAR(Cl)$_4$ follows a specific protocol that is detailed in the sections below. Figure 2-1 below is a scheme of the synthesis protocol.

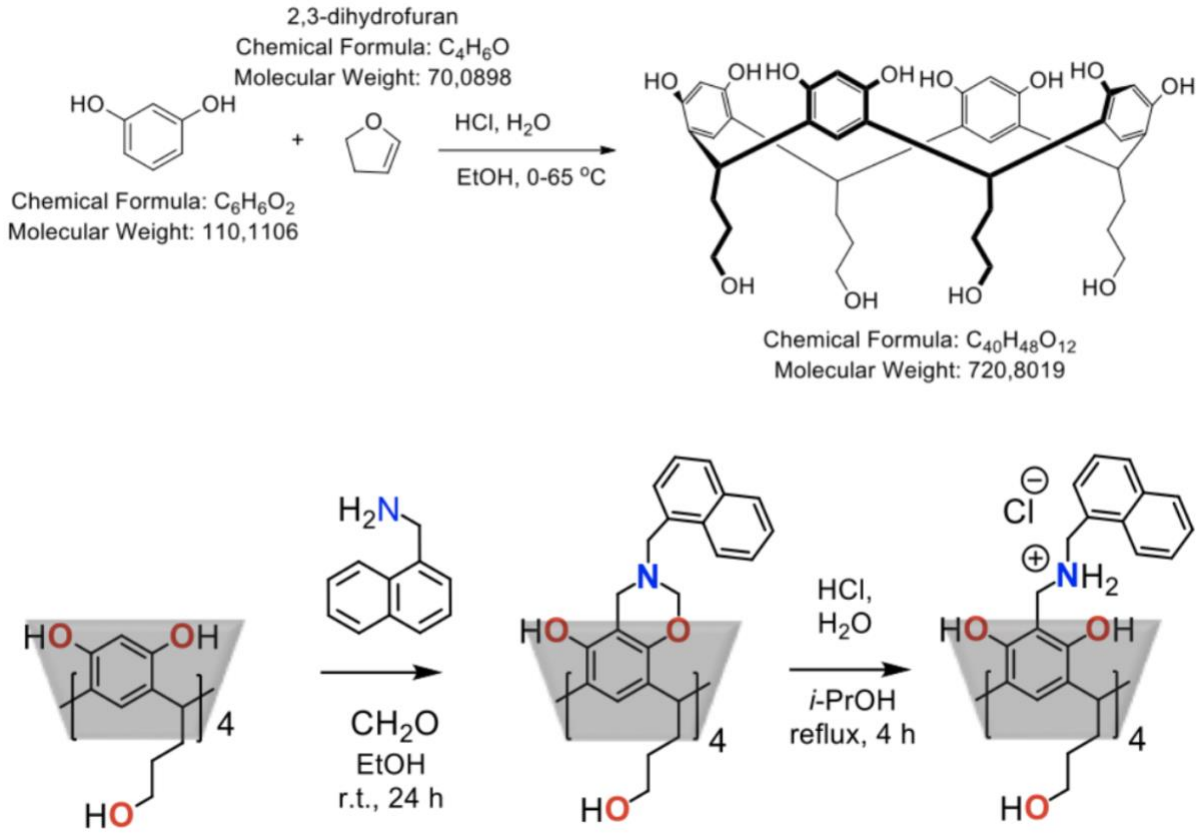

Figure 2-1: Overview of Np-NAR(Cl)$_4$ synthesis from resorcinol.

2.1 FORMATION OF RING AND LOWER RIM HYDROXYLATION

To obtain the hydroxylated lower rim resorcin[4]arene, dissolve 20.0 grams (g) of resorcinol in 150 milliliters (mL) of 4:1 methanol/37% hydrochloric acid (HCl) solution. Add 13.8 mL of 2,3-dihydrofuran via syringe pump to the system over 4 hours. Allow the mixture to stir for an additional 4 hours before heating to 50 degrees Celsius and leaving to stir for 7 days. Filter off the resulting precipitate and take up 2 liters (L) of cold distilled water. Filter off the solid again and allow it to dry under vacuum at room temperature overnight. Confirm the product via NMR in DMSO-d_6 solvent. Wash further with dry tetrahydrofuran (THF) if necessary.

2.2 ADDITION OF UPPER RIM NAPHTHALENE GROUP

To form the *N*-naphthyl ammonium tetra benzoxazine, add 5.0g of hydroxylated resorcinarene, 28 mL of 36% formaldehyde, and 60 mL methanol to a round bottom flask. Next, very slowly drip 4.25 mL of 1-naphthylmethylamine in 15 mL ethanol and then into the initial mixture at room temperature. Stir for 24 hours after all the reagents are added. The solid is filtered off and dried under vacuum. Recrystallization in methanol/n-hexane solution may be added as a purification step if a clean NMR is not obtained.

2.3 CREATION OF FINAL SALT

Forming the final Np-NAR$(Cl)_4$ salt requires the following steps:

2.3.1 REFLUX

- In a fume hood, isolate 0.5 g of intermediate 4B into a round bottom flask. To the flask, add 2 mL deionized water, 25 mL isopropanol, and 1.5 mL of a *diluted acid mixture* (this mixture consists of 1.5 mL concentrated 37% HCl added to 1.5 mL deionized water). In addition, place a stir bar into the flask to ensure proper mixing during the reflux. Set up reflux apparatus, so that cold water is constantly flowing which will allow for condensation of vapors. Attach the round bottom flask to the reflux apparatus using clips and submerge the bottom into an oil bath on a hot plate. Heat to 90 degrees Celsius and leave the reflux running for 4 hours. Then, pull the flask from the oil bath and allow it to cool to room temperature naturally.

2.3.2 AZEOTROPIC DISTILLATION

- Add approximately 50 mL of chloroform to the flask and attach it to a distillation apparatus which includes a two necked glassware attachment with the vertical portion paired with a thermometer and the horizontal portion paired with a reflux condenser. At the end of the reflux condenser, a curved neck attachment will be positioned over an empty beaker. Refer to Figure 2-2 for visualization of the azeotropic distillation setup. Emerge the round bottom flask in the oil bath and heat to 100 degrees Celsius. Wait for the chloroform to pull out excess formaldehyde and water from the product. The beaker will fill up with approximately 50mL, or the original amount of chloroform added to the system.

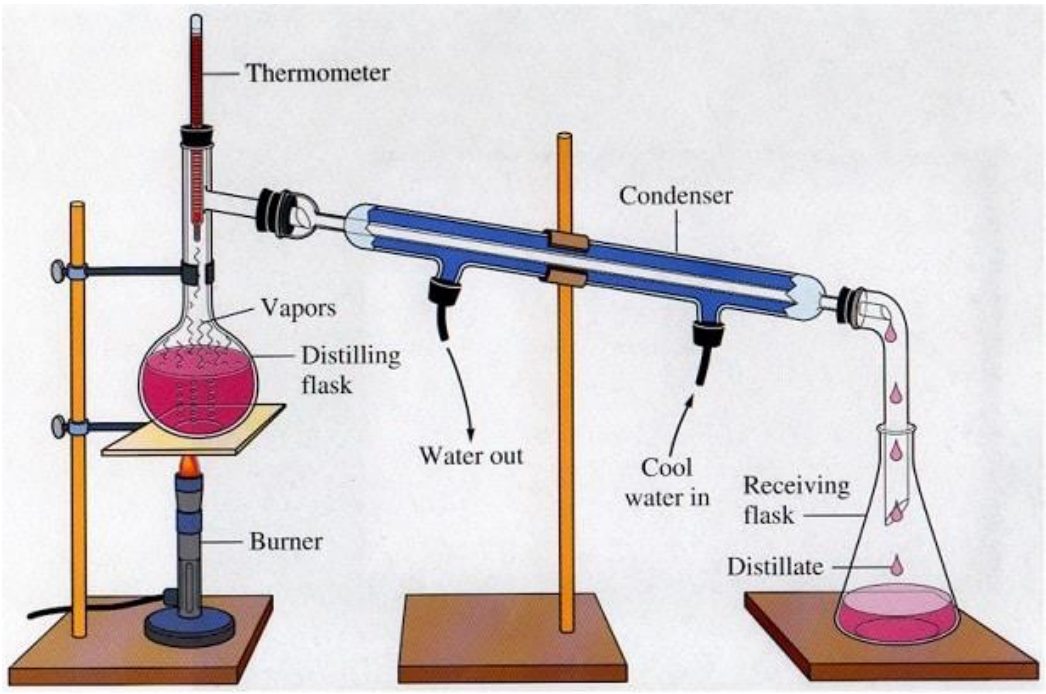

Figure 2-2: Setup of azeotropic distillation apparatus. Acquired from reference.[46]

2.3.3 ROTARY EVAPORATION

- Get the setup oriented so that your round bottom flask is submerged in the water and attached to the apparatus. Figure 2-3 illustrates the setup. Increase the temperature to 80 degrees Celsius and spin slowly (setting 30). Subsequently increase the pressure so that the extra solvent evaporates, but not too fast where you lose product. Once the solvent is entirely evaporated, remove the flask from the water and scrape the crystals off the sides of the flask with a spatula.

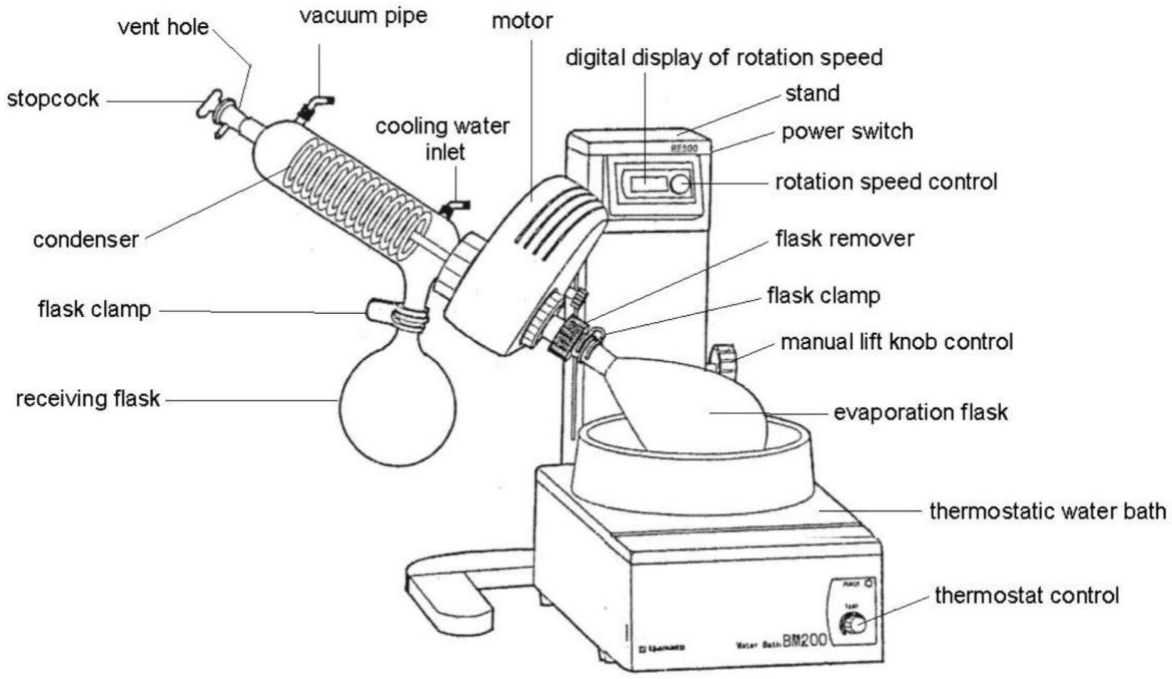

Figure 2-3: Rotary evaporation setup. Acquired from reference.[47]

2.3.4 RECRYSTALLIZE

- This step takes place in the fume hood. When most of the product has been scraped from the sides of the flask, add diethyl ether. Swirl the flask and dump the contents into a vacuum filtration apparatus (side arm flask and Buchner funnel). Repeat this until all the product is removed from the round bottom flask. Diethyl ether evaporates very quickly, so your crystals should reappear in the funnel. Allow them to dry completely. Place into a smaller round bottom flask and dry under nitrogen gas if necessary.

2.3.5 CONFIRMATION OF PRODUCT

- Take a small amount of the product into an NMR tube and add either methanol d-4 or dimethyl sulfoxide d-6 (MeOD or DMSO-d_6). Record which solvent you use for reference on the NMR spectrum.
- Run 16 scans and analyze the spectra to confirm that you have obtained the desired product.

2.4 COMMENTS ON COST EFFECTIVENESS

From Figure 2-1, synthesis of 3-hydroxyl resorcinarene from resorcinol and 2,3 dihydrofuran can be done in large quantities with very high percentage yields. Optimizing the synthesis procedures allows optimizing the cost effectiveness of synthesizing the receptor.

1. First, only proceed with purification steps if needed. If a clean confirmation NMR is obtained for a particular intermediate or final product that has been created, there is no need to go ahead with a purification. This will waste time and lead to overall decreased yields of the final product because some will be lost in glassware. Furthermore, purification steps require that another confirmation NMR run to visualize the improvements. This will reduce the amount of viable product as well.
2. Second, decreasing the amount of glassware used can prevent loss of product stuck to the sides of round bottom flasks that are difficult to get.
3. Finally, do not use too much concentrated acid in the last step to make the salt as that can degrade the entire product and intermediate.

2.5 JUSTIFICATION FOR NAPHTHALENE FUNCTIONALIZATION OF THE RESORCIN[4]ARENE CORE

The upper rim naphthalene functionalization has been proven to have the optimal degree of hydrophobicity and aromaticity to interact with KynA at a molecular level. Computational analysis performed using the Grimme's dispersion-corrected functional, B3LYP-D3-derived optimized geometries of the host-KynA system justifies this pi-pi stacking interaction between the two molecular species as well as the host acting as a hydrophobic haven for KynA in a mostly polar environment. KynA binding was compared between an upper rim benzene resorcinarene and upper rim naphthalene resorcinarene using NMR chemical shift analysis in addition to ITC thermodynamic evaluation. The results indicate benzene functionalization did not induce as strong of an interaction to KynA as naphthalene. Pyrene upper rim functionalized resorcinarene was also compared to naphthalene in a similar fashion using NMR and ITC screening, but again the interaction with KynA was not as strong as with naphthalene. All resorcinarene structures are shown in Figure 2-4. The highest affinity functionalized resorcinarene is desirable because strong binding to biomolecules makes a sufficient organic sensor as the physiological concentrations become minuscule.[48] This sensor must be able to strongly interact with KynA even at very small physiological and pathological concentrations. Figure 2-5 summarizes the NMR and ITC data to justify the receptor choice.

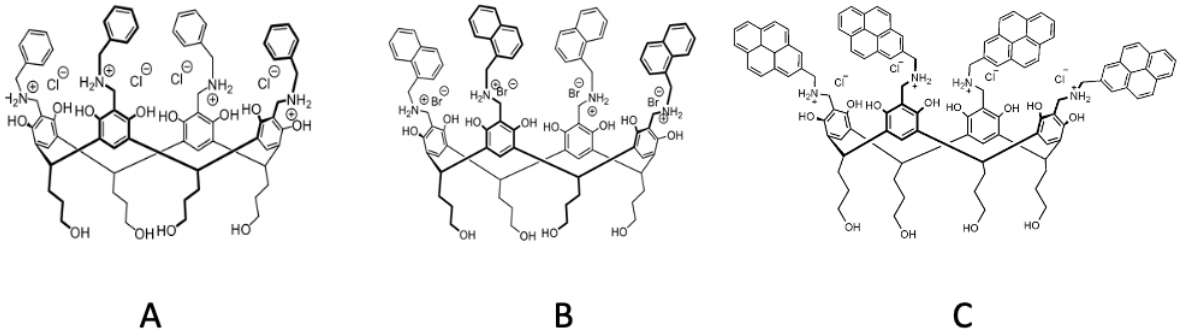

Figure 2-4: (A) Structure of upper rim functionalized benzene resorcinarene, (B) Structure of upper rim functionalized naphthalene resorcinarene, (C) Structure of upper rim functionalized pyrene resorcinarene.

Receptor	Aromatic Peak Chemical Shift Change (Degree of Shielding) (NMR)	K_a x 10^3 (M^{-1}) (ITC)
Benzene (Figure 2-4A)	+0.51 ppm	2.3
Naphthalene (Figure 2-4B)	+0.12 ppm	4.8
Pyrene (Figure 2-4C)	+0.00 ppm	No binding

Figure 2-5: NMR chemical shift & ITC binding constant summarized for the three receptors.

2.6 SUMMARY OF INTERACTION ANALYSIS

Interaction analysis is a series of analytical methods that determine which host functionalization is optimal for host-guest interactions. This process begins with qualitative analysis using NMR. Three samples are prepared- (1) pure KynA, (2) pure host (3) KynA-host mixture. Chemical shift analysis of these NMR spectra reveals whether binding is occurring between the species. Binding can be displayed through broadening of pure KynA or pure host peaks in the mixture's spectra as well as up field movement along the x axis indicating a change in the chemical environment of the hydrogens- only accomplished by binding. Figure 2-6 and Figure 2-7 are examples of NMR spectra for hosts that clearly bind or do not bind with KynA, respectively.

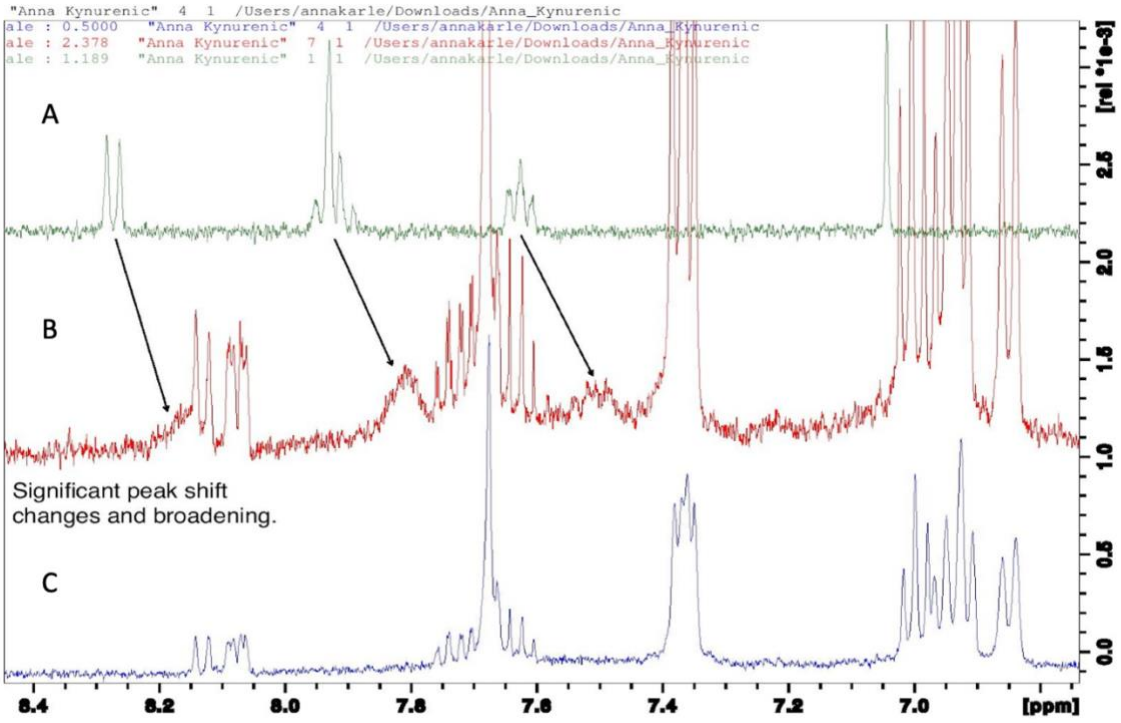

Figure 2-6: NMR spectra stacked and analyzed for a host that does indicate binding with KynA, Np-NAR(Cl)$_4$. Top to bottom: (A) Pure KynA scan, (B) mixture of KynA and Np-NAR(Cl)$_4$, (C) Pure Np-NAR(Cl)$_4$ scan.

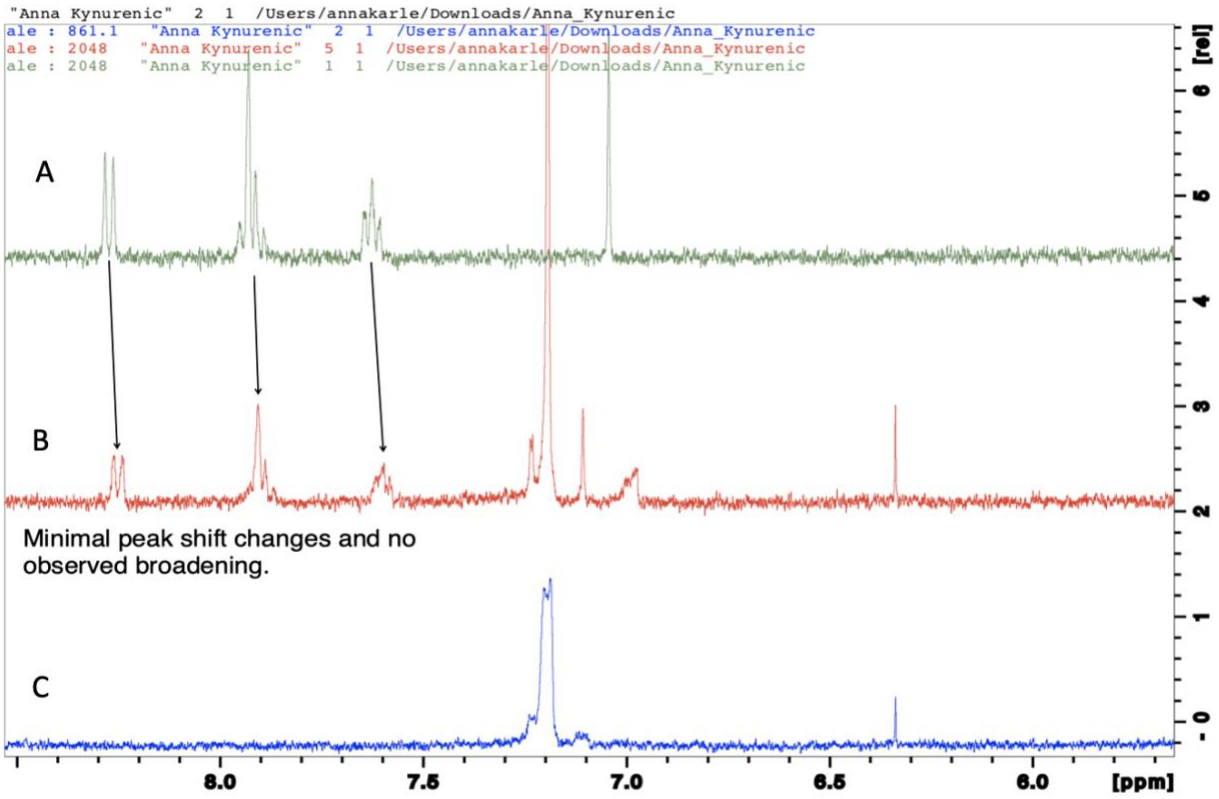

Figure 2-7: NMR spectra stacked and analyzed for a host that does not indicate binding with KynA. Top to bottom: (A) Pure KynA scan, (B) mixture of KynA and nonbinding host, (C) Pure host scan.

Once binding within the system is confirmed qualitatively, ITC allows quantification of the binding by providing thermodynamic values including enthalpy and entropy as well as the binding constant for the system. This involves creating a concentrated guest solution to titrate via syringe into a cell of less concentrated host. Tracking the thermodynamics of the cell as the injections progressess allows quantification of the binding process. Figure 2-8 shows the binding constant and titration curve for the system between the naphthalene host and KynA.

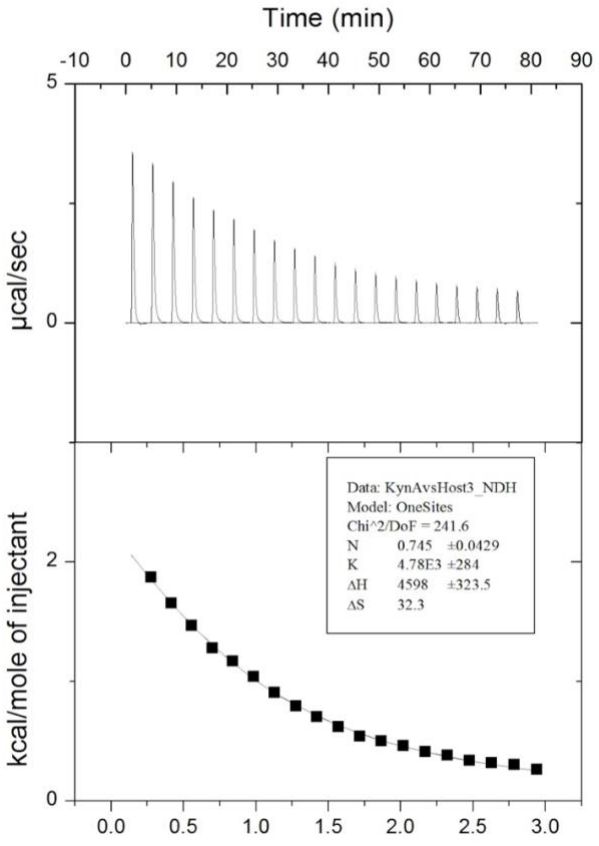

Figure 2-8: ITC data including titration curve and binding constant for the system between KynA and Np-NAR(Cl)$_4$.

After ITC quantification, Ultraviolet/Visible Spectroscopy (UV-Vis) and Fluorescence Spectroscopy are used to further evaluate the binding affinity through a series of titration experiments. After extensive searching of multiple different functionalized resorcinarenes (Figure 2-9), Np-NAR(Cl)$_4$ was determined to be optimal for sensing KynA due to its high affinity and selectivity. Figures 2-6 and 2-8 justify this conclusion by qualitatively and quantitatively expressing the strength of binding via NMR and ITC, respectively.

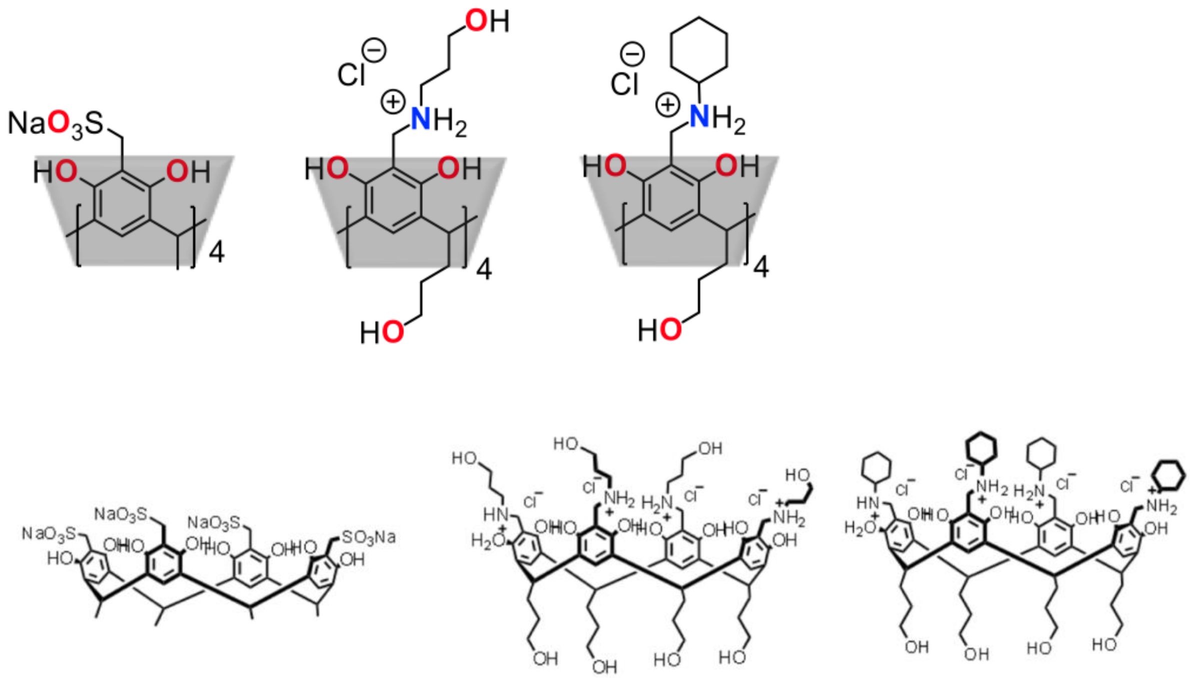

Figure 2-9: Other proposed hosts, condensed and expanded forms.

CHAPTER 3

3.0 QUANTIFYING HOST SENSITIVITY FOR KYNURENIC ACID

3.1 INSTRUMENTATION

Ultraviolet-visible (UV-Vis) spectroscopy experiments were performed on an Agilent Cary-100 spectrophotometer. Fluorescence experiments were performed using a Horiba Jobin-Yvon Fluorolog 3 with scans being run with an experimentally determined optimal excitation wavelength of 475 nm.

3.2 SAMPLE PREPARATION

UV samples were prepared in 30/70 DMSO/H_2O for complete solubility. Np-NAR$(Cl)_4$ was prepared at 3mM concentration and KynA was prepared at 50mM concentration. These solutions were utilized in a titration of KynA against a starting sample of 3mL pure Np-NAR$(Cl)_4$ in increments of 20 microliters (µL) until the end when the solution was saturated in an excess of KynA. This titration was performed twice to confirm the reproducibility and accuracy of the first dataset.

Physiological concentration of KynA is too small for the Agilent Cary-100 spectrophotometer to detect, so fluorescence spectroscopy was utilized for the KynA-Np-NAR$(Cl)_4$ interaction. For sample preparation, a 1:2 (human plasma: deionized water) solvent was prepared using 5 mL freeze dried human plasma bought from Sigma Aldrich and 10 mL deionized water. A 1 mM solution of KynA was prepared in the plasma solvent and diluted to 0.01 mM to act as the titrant. A 5 mM solution of Np-NAR$(Cl)_4$ was prepared in the plasma solvent to serve as the titrand.

3.3 ULTRAVIOLET-VISIBLE SPECTROSCOPY TITRATIONS

UV-Vis spectroscopy can display any absorbance peak(s) between 200 and 800 nanometers (nm), exposing the aromaticity and conjugated pi (π) bonds of a particular molecule. Once a calibration curve is obtained for a specific molecule with an R^2 value close to 1, UV can be used for quantitative estimation of concentration. The absorbance of a solution with an unknown concentration can be found experimentally by extrapolating from the calibration curve.

For titrations, the host solution of Np-NAR$(Cl)_4$ was placed in a two-side frosted cuvette and run as a pure sample after a baseline is obtained. The max absorbance peak for Np-NAR$(Cl)_4$ was identified at 515 nm, experimentally. Small amounts (see Figure 3-1 for details) of 0.01 mM stock solution of KynA were titrated into the frosted cuvette containing an initial 3 mL of Np-NAR$(Cl)_4$. The absorbance was immediately scanned after the titration was complete. Throughout the titration, the 515 nm host peak gradually increased in absorbance intensity as KynA saturated the system as seen in Figure 3-2. Titrating in KynA to the host system will cause movement of the host absorbance peak if binding interactions are occurring between the two species. Indeed the interaction causes movement in the absorbance peaks of the receptor. UV-Vis has limitations as it is unable to detect very small concentrations of titrant in solution, so fluorescence spectroscopy experiments are coupled with this method to supplement our knowledge of the host guest interactions in physiological concentrations.

Figure 3-3 introduces another interesting note to consider as KynA is replaced with Trp under the same conditions. This system shows no peak movement when Trp is titrated into Np-NAR$(Cl)_4$.

Spectrum No.	**1**	2	3	4	5	6	7	8	9	10	11	12	13	14	15	16	17
Equiv. added Kyn guest	**0.00**	0.01	0.02	0.04	0.07	0.10	0.14	0.18	0.21	0.25	0.29	0.33	0.38	0.49	0.64	0.84	1.09
Addition of KynA guest in uL:	**-**	1.00	2.00	5.00	5.00	5.00	7.00	7.00	7.00	7.00	7.00	7.00	10.0	20.0	30.0	40.0	50.0
Total volume of KynA added in uL	**-**	1.00	3.00	8.00	13.0	18.0	25.0	32.0	39.0	46.0	53.0	60.0	70.0	90.0	120.0	160.0	210.0
Total volume in Cuvette in uL	**3000.0**	3001.0	3003.0	3008.0	3013.0	3018.0	3025.0	3032.0	3039.0	3046.0	3053.0	3060.0	3070.0	3090.0	3120.0	3160.0	3210.0
Total concentration of KynA guest	**0.00**	0.00001666	0.00004995	0.00013298	0.00021573	0.00029821	0.00041322	0.00052770	0.00064166	0.00075509	0.00086800	0.00098039	0.00114007	0.00145631	0.00192308	0.00253165	0.00327103

Figure 3-1: Details of UV-Vis titration experiment.

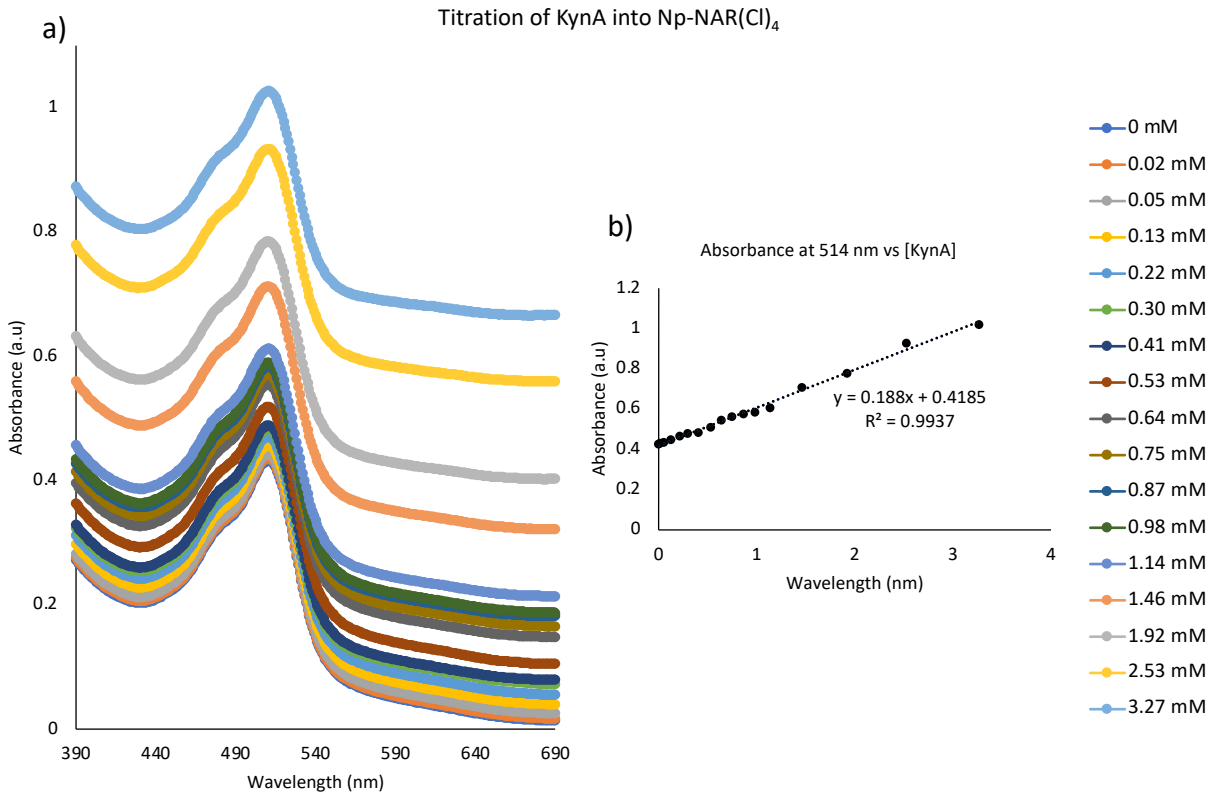

Figure 3-2: UV-Vis spectroscopy data for KynA titrations against Np-NAR(Cl)$_4$

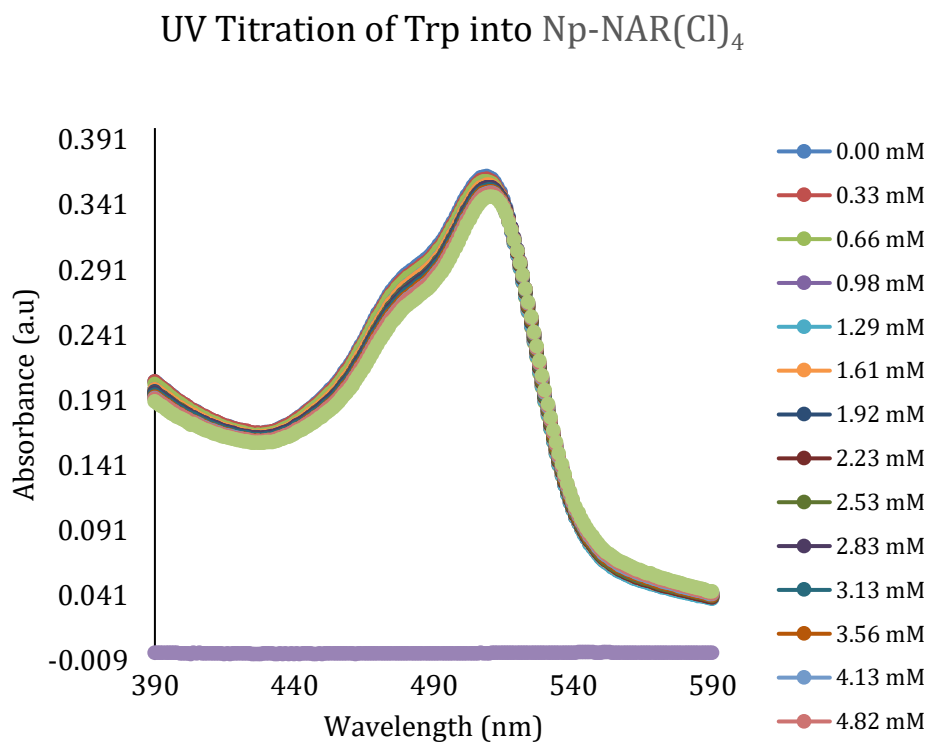

Figure 3-3: UV-Vis spectroscopy data for Trp against Np-NAR(Cl)$_4$

3.4 FLUORESCENCE SPECTROSCOPY TITRATIONS

Fluorescence spectroscopy displays both excitation and emission wavelengths across the range of 200 to 800 nm for conjugated systems. This method is much more sensitive than UV-Vis spectroscopy, so it is often used in experiments to visualize host-guest interactions in physiological as well as pathological ranges. Experimentally, an excitation wavelength of 475 nm was the ideal parameter for producing emission spectra. The results of the titration displayed in Figure 3-3 shows a fascinating phenomenon called quenching. As KynA increases in equivalence to Np-NAR(Cl)$_4$, the emission signal begins to decrease in intensity. Quenching indicates host guest binding in the small physiological concentration; this means that the sensing ability of the organic host for KynA is satisfactory for clinical tests because the interactions occur even in such tiny concentrations.

This indicates that Trp metabolism must occur before the host will develop any interactions. The purpose of this Trp titration experiment is to rule out the possibility of falsely high clinical lab results. Trp must break down into KynA in physiological substances, such as human blood plasma, before the Np-NAR(Cl)$_4$ host senses KynA at all.

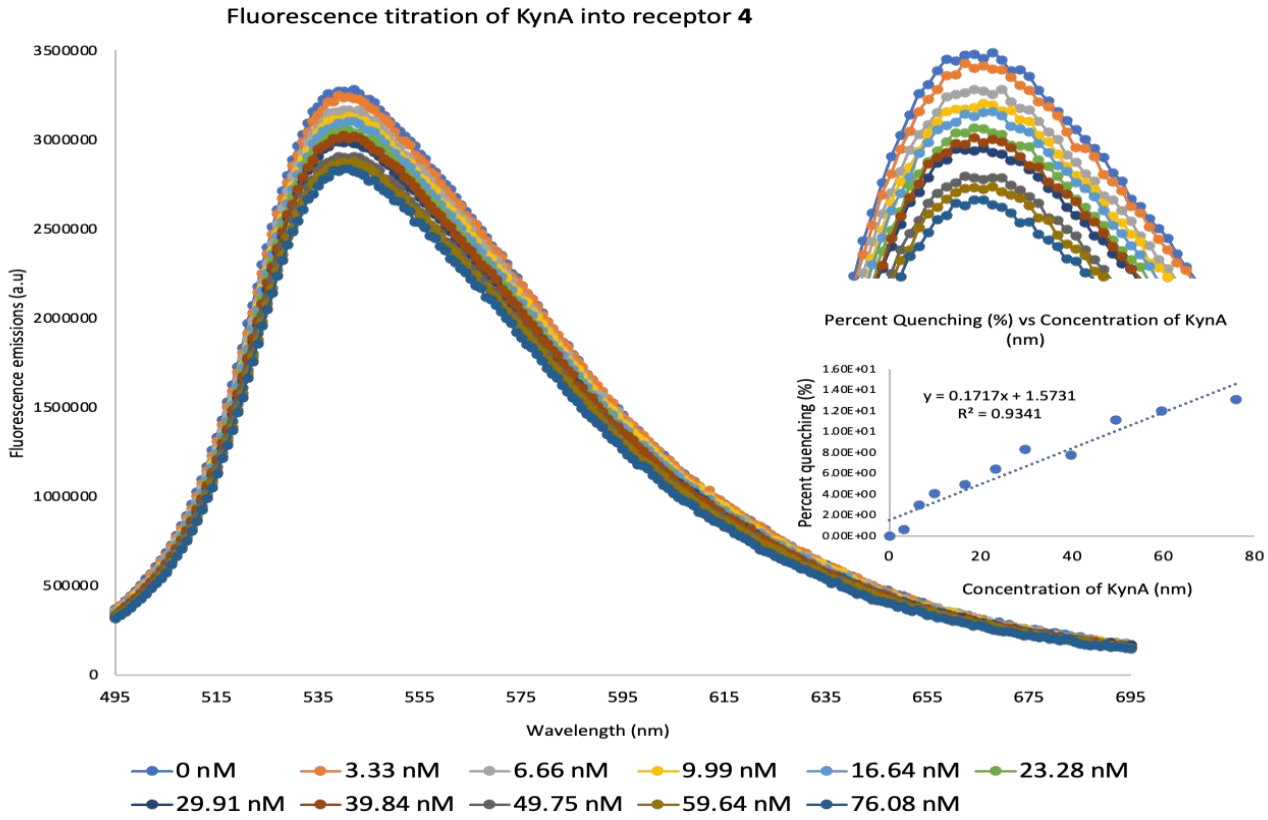

Figure 3-4: Fluorescence KynA signal in physiological concentration against Np-NAR(Cl)$_4$ in water, quenching details.

CHAPTER 4

4.0 EVALUATION OF HOST SELECTIVITY FOR KYNURENIC ACID

Not only is it important to prove that our host can sense a molecule in certain media and ranges of concentrations, but it also must be able to discriminate between its target molecule and others, most notably metabolites or precursors. This chapter will explore the host's ability to distinguish KynA from Trp, its precursor. In the context of KynA, a summary of Trp metabolism is outlined in Figure 4-1. This figure emphasizes the importance of host selectivity by showing how Trp metabolism follows the kynurenine pathway, resulting in the production of KynA. Inaccurate test results, such as false positives, are inevitable in many biosensors. An abundance of these inaccuracies, however, can be avoided through the confirmation of sensitivity for the specific biomolecule as opposed to its precursors or metabolites.

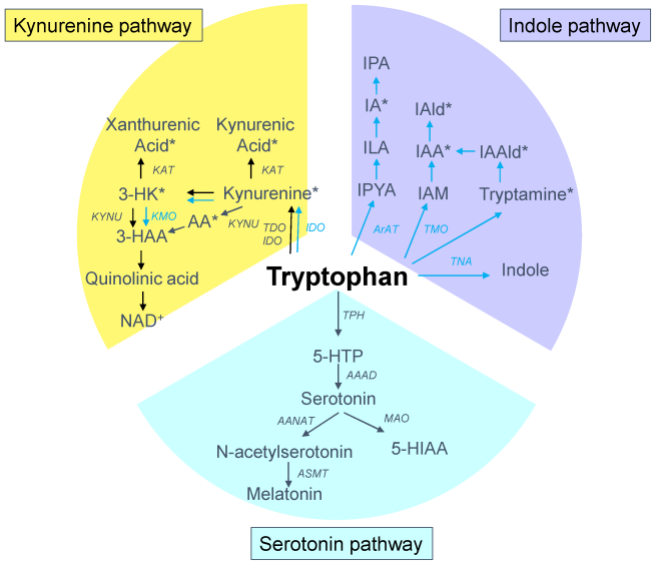

Figure 4-1: Overview of tryptophan metabolism including the kynurenine pathway. Adapted from reference.[50]

4.1 INSTRUMENTATION

The selectivity experiments were conducted using Bruker Avance 200 MHz NMR.

4.2 SAMPLE PREPARATION

Stock solutions of KynA (2 mM) and Trp (2 mM) were prepared in 70% D_2O and 30% DMSO-d_6. A 1:1 mixture of KynA: Np-NAR(Cl)$_4$ was created by pipetting 250 μL of KynA and 250 μL of Np-NAR(Cl)$_4$ into the same NMR tube. Similarly, a 1:1 mixture of Trp: Np-NAR(Cl)$_4$ was made in a different NMR tube using the same parameters.

4.3 COMPETITION EXPERIMENTS

First, KynA and Trp were evaluated separately against the host. Figure 4-2 shows qualitative binding between KynA and Np-NAR(Cl)$_4$ through aromatic KynA peak broadening and chemical shift changes. The movement of peaks is relative from the pure KynA sample to the mixture with the host. Trp was evaluated in the same way but showed negligible movement. In this way, it is concluded that there is minimal binding between Trp and the host which means metabolism must occur before the host will identify KynA in the body. The host selectivity for KynA appears to be concrete from this experiment alone.

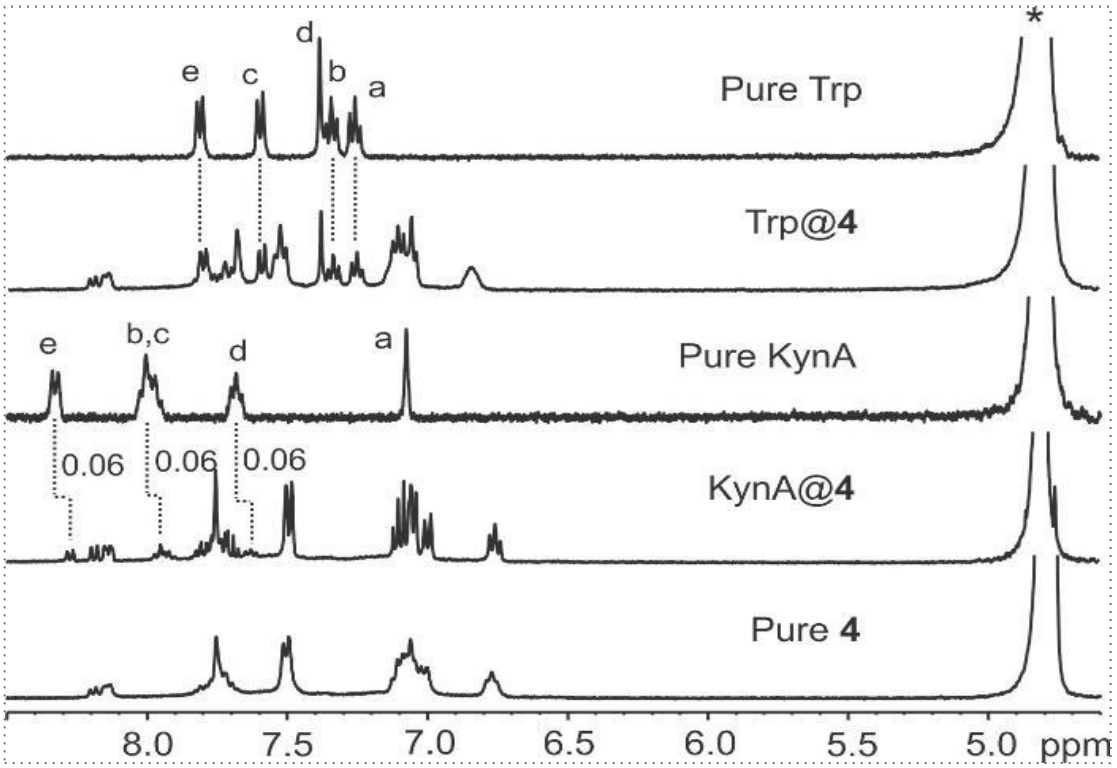

Figure 4-2: Qualitative analysis of Trp-host binding compared to KynA-host binding in NMR. Np-NAR(Cl)$_4$ host labeled **4** as it was the 4th host to be tested for KynA affinity.

To prove the host's selectivity for KynA over Trp, however, another NMR competition experiment was carried out in which Trp saturated the system when compared to KynA. The host was titrated into the tube over the course of 5 titrations increasing in 0.2 increments of equivalence to KynA. This allowed for observation of the system between 0 and 1.0 equivalence of host to KynA. Figure 4-3 display the results of this experiment. As expected, according to the previous findings, an excess of Trp in the tube did not make a difference in binding selectivity or affinity. Despite the large excess of Trp in the system, the host continued to bind exclusively and strongly with KynA. This experiment furthermore solidifies the argument of the selectivity Np-NAR(Cl)$_4$ host has for KynA in the presence of its precursor.

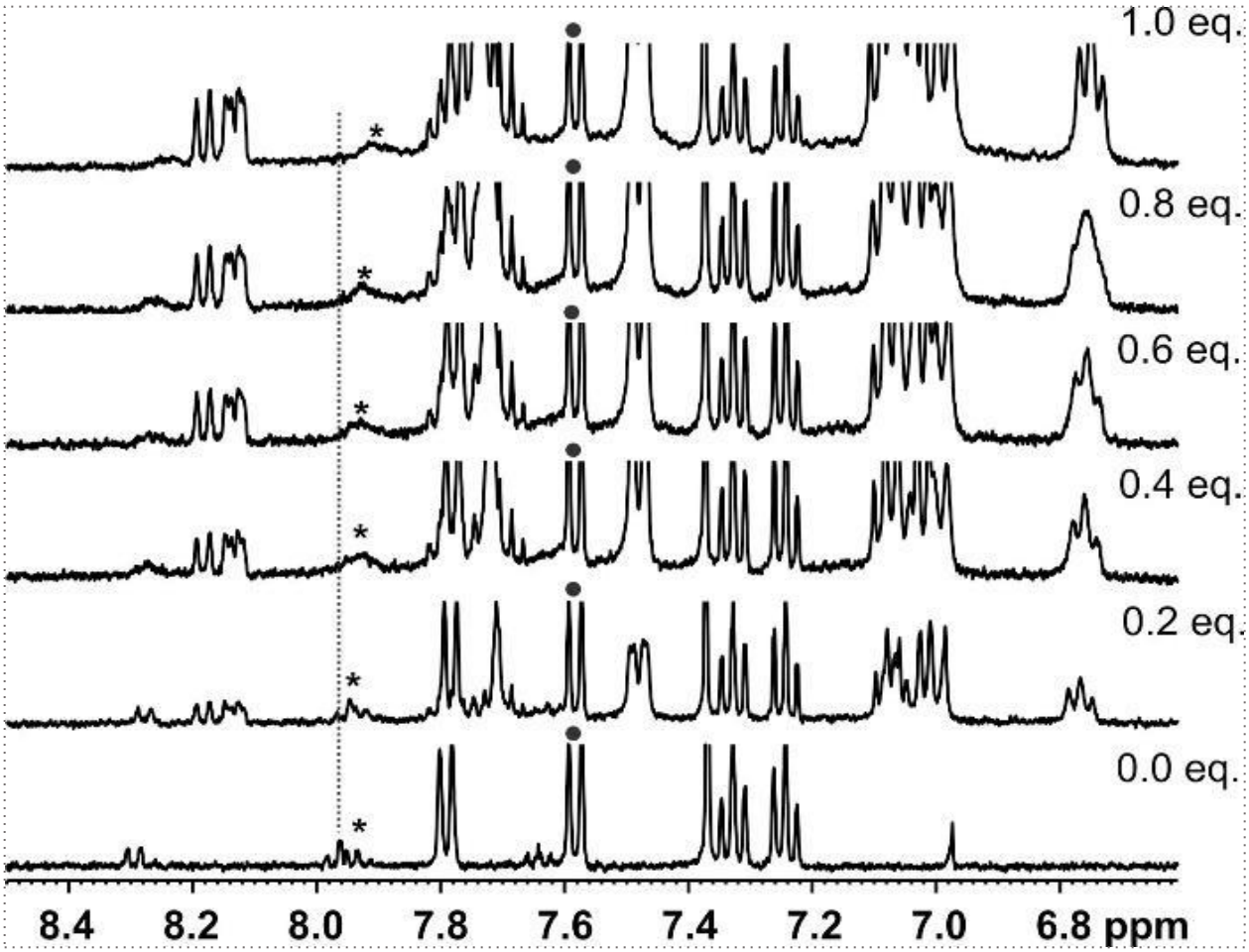

Figure 4-3: Trp competition experiment. The star represents the aromatic KynA peaks that are involved in binding with the host. Note the movement and broadening of the peak with an increasing equivalence of the host. The dot represents the Trp peak that would be involved in binding with the host, but clearly does not even with a completely saturated Trp system.

Proof that the sensor has no affinity towards Trp will reduce the number of incorrect lab results, particularly false positives. These false positives would indicate that a patient has abnormally high KynA concentrations when the host is just binding Trp in addition to KynA. Nonselective binding would lead physicians to assume higher levels of KynA in the body and disregard the chance of depression predisposition or overestimate the likelihood of schizophrenia development.

CHAPTER 5

5.0 EVALUATION OF HOST-GUEST COMPLEX STABILITY

5.1 INSTRUMENTATION

The stability experiment was conducted over nine (9) weeks using Bruker Avance 200 MHz NMR.

5.2 SAMPLE PREPARATION

Stock solutions of KynA (2 mM) and Np-NAR(Cl)$_4$ (2 mM) were prepared in 70% D_2O and 30% DMSO-d_6. For a 1:1 (KynA: Np-NAR(Cl)$_4$) mixture, 250 μL of KynA and 250 μL of Np-NAR(Cl)$_4$ were pipetted into a clean NMR tube making an equimolar sample concentration in the mixture.

5.3 PROTON NUCLEAR MAGNETIC RESONANCE STABILITY EXPERIMENTS

The host-guest complex was monitored weekly at 25 degrees Celsius over 9 weeks. Solvent peaks were calibrated after scans were complete so that each week's spectra were calibrated according to the majority solvent which allowed accurate analysis of the observed movement of the aromatic peaks (~7-8ppm) without the risk of misrepresenting the data acquired. Figure 5-1 illustrates the results of the stability experiment with each week's spectra identified, including a pure KynA spectrum located at the top and a pure Np-NAR(Cl)$_4$ spectrum at the bottom. During the analytical phase of this experiment, the aromatic KynA peaks were tracked over time. Observations to note include the week 9 finding where it is seen that the aromatic signals were completely deshielded and they appear identical to the chemical shifts seen in the pure KynA spectra (blue spectra). Another observation to note is that the Np-NAR(Cl)$_4$ peaks continue to move downfield as the

weeks progress. These peaks represent an average of the different chemical species. Both of these observations lead us to the same conclusion that around 4 weeks the host-guest compound begins to self-aggregate.

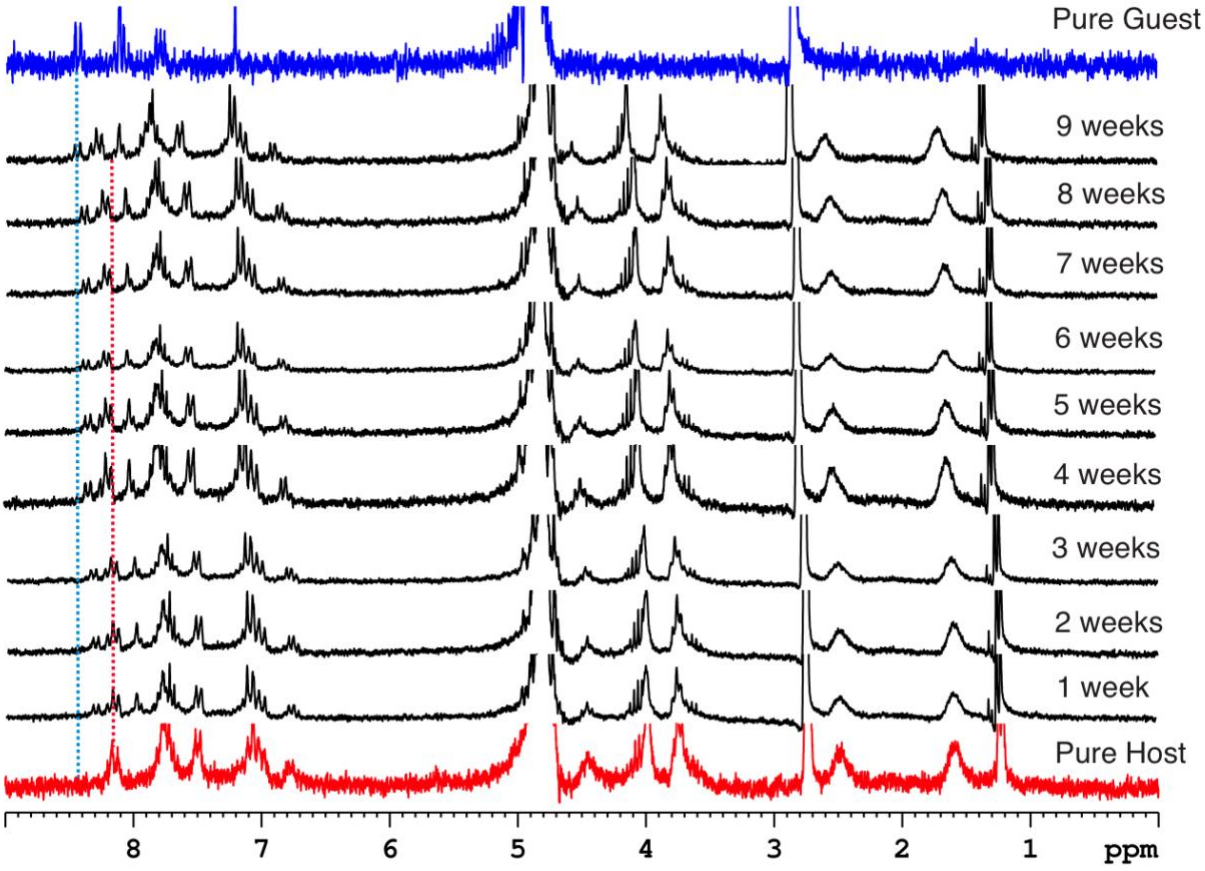

Figure 5-1: Stability KynA-Np-NAR(Cl)$_4$ NMR screenings, weeks 1-9. Blue spectrum is a sample of pure KynA. Red spectrum is a sample of pure Np-NAR(Cl)$_4$.

5.4 CLINICAL IMPLICATIONS FOR STABILITY

The longevity of a host-guest complex is critical to its success to act as a biosensor. If the complex degrades within hours, or even days, it is often difficult for an inpatient or outpatient laboratory to prioritize a clinically nonurgent specimen due to the volume of the other time sensitive specimens received. In a hospital setting, emergency department tests (troponin, for example) that are ordered

for patients suspected to be experiencing myocardial infarctions or other life-threatening complications take up most stat orders. A non-urgent susceptibility test that could indicate a patient's predisposition to develop various forms of depression, which is outlined in this thesis, does not take priority over emergent diagnostic testing. The routine test orders would be better integrated into a laboratory if the complex can maintain stability over a longer period. Seeing that the KynA-Np-NAR$(Cl)_4$ complex is stable in solution for nearly a month, a patient's blood sample for this test would be expected to maintain stability for a similar amount of time. This means that the complex will not rapidly degrade when Np-NAR$(Cl)_4$ is introduced into the blood sample.

Additionally, stability of a host-guest complex is important logistically when it comes to interpreting the results of a test. The results of the test will be accurate for an acceptable window of time without having to be processed under stat priority as a time sensitive test, which is not ideal as discussed above. Degradation of the complex could produce misleading results and in turn, misleading diagnoses of patients. False positives for depression predispositions would be the most typical conclusion of inaccurate results because lower levels of KynA have been associated with depression. If the host dissociates with the KynA in the blood, even if there is a normal physiological level for a particular patient, the fluoroscopy test will show low levels of KynA bound to the host. This lab result would most likely lead a physician to proceed with the interpretation that the patient has low KynA levels and thus may develop depression at a higher incidence than a patient with normal KynA levels. The stability of the complex makes a stronger case for the test's practical ability to be standardized in the medical community's laboratories.

CHAPTER 6

6.0 CONCLUSION

Mental health disorders take a disastrous toll on patients as well as the American healthcare system, costing billions of dollars annually to accommodate these diseases.[51] Identifying biomarkers that reliably predict mental health disorders will allow physicians and clinical staff to get a head start on treating patients with major depressive disorder or schizophrenia. This will change the way we manage patients in an outpatient clinic and prevent them from ending up in an inpatient setting due to their illness. Our findings concluded that the naphthalene functionalized resorcinarene receptor is capable of high affinity and selective binding for KynA.[33] Further investigation of binding in the experiments discussed in this thesis focused primarily around establishing the host's ability to function in a clinical setting. Evaluation of the host's sensitivity in physiological concentration as well as stability in solution over time was critical in the host's success as a biosensor. The ability to detect KynA in its physiological range in human plasma was confirmed by fluorescence spectroscopy and the stability of the host-guest complex was observed by NMR over several months. Considering the growing interest in personalized medicine, this biosensor recognition element has the potential to serve the medical community as a diagnostic predictor for patients who may develop a variety of psychological conditions.

6.1 ACKNOWLEDGEMENTS

Words truly cannot express my overwhelming gratitude for my PhD mentor, Kwaku Twum, for all of his support and insight through this process. I owe so much of my success and perserverance to him. I am incredibly thankful for Dr. Ngong Kodiah Beyeh and the Provost award for the resources to conduct research and to the SURP program for expanding my opportunity to learn and grow as a scientist.

REFERENCES

(1) Tóth, F.; Cseh, E. K.; Vécsei, L. Natural Molecules and Neuroprotection: Kynurenic Acid, Pantethine and α-Lipoic Acid. *International Journal of Molecular Sciences 2021, Vol. 22, Page 403* **2021**, *22* (1), 403. https://doi.org/10.3390/IJMS22010403.

(2) Szalardy, L.; Zadori, D.; Toldi, J.; Fulop, F.; Klivenyi, P.; Vecsei, L. Manipulating Kynurenic Acid Levels in the Brain – On the Edge Between Neuroprotection and Cognitive Dysfunction. *Current Topics in Medicinal Chemistry* **2012**, *12* (16), 1797–1806. https://doi.org/10.2174/156802612803989264.

(3) Moroni, F.; Cozzi, A.; Sili, M.; Mannaioni, G. Kynurenic Acid: A Metabolite with Multiple Actions and Multiple Targets in Brain and Periphery. *Journal of Neural Transmission* **2012**, *119* (2), 133–139. https://doi.org/10.1007/S00702-011-0763-X/FIGURES/4.

(4) Ruddick, J. P.; Evans, A. K.; Nutt, D. J.; Lightman, S. L.; Rook, G. A. W.; Lowry, C. A. Tryptophan Metabolism in the Central Nervous System: Medical Implications. *Expert Reviews in Molecular Medicine* **2006**, *8* (20), 1–27. https://doi.org/10.1017/S1462399406000068.

(5) Gostner, J. M.; Geisler, S.; Stonig, M.; Mair, L.; Sperner-Unterweger, B.; Fuchs, D. Tryptophan Metabolism and Related Pathways in Psychoneuroimmunology: The Impact of Nutrition and Lifestyle. *Neuropsychobiology* **2020**, *79* (1–2), 89–99. https://doi.org/10.1159/000496293.

(6) Plitman, E.; Iwata, Y.; Caravaggio, F.; Nakajima, S.; Chung, J. K.; Gerretsen, P.; Kim, J.; Takeuchi, H.; Chakravarty, M. M.; Remington, G.; Graff-Guerrero, A. Kynurenic Acid in Schizophrenia: A Systematic Review and Meta-Analysis. *Schizophrenia Bulletin* **2017**, *43* (4), 764–777. https://doi.org/10.1093/SCHBUL/SBW221.

(7) Kindler, J.; Lim, C. K.; Weickert, C. S.; Boerrigter, D.; Galletly, C.; Liu, D.; Jacobs, K. R.; Balzan, R.; Bruggemann, J.; O'Donnell, M.; Lenroot, R.; Guillemin, G. J.; Weickert, T. W. Dysregulation of Kynurenine Metabolism Is Related to Proinflammatory Cytokines, Attention, and Prefrontal Cortex Volume in Schizophrenia. *Molecular Psychiatry 2019 25:11* **2019**, *25* (11), 2860–2872. https://doi.org/10.1038/s41380-019-0401-9.

(8) Carlborg, A.; Jokinen, J.; Jönsson, E. G.; Erhardt, S.; Nordström, P. CSF Kynurenic Acid and Suicide Risk in Schizophrenia Spectrum Psychosis. *Psychiatry Research* **2013**, *205* (1–2), 165–167. https://doi.org/10.1016/J.PSYCHRES.2012.08.021.

(9) Sellgren, C. M.; Gracias, J.; Jungholm, O.; Perlis, R. H.; Engberg, G.; Schwieler, L.; Landen, M.; Erhardt, S. Peripheral and Central Levels of Kynurenic Acid in Bipolar Disorder Subjects and Healthy Controls. *Translational Psychiatry 2019 9:1* **2019**, *9* (1), 1–9. https://doi.org/10.1038/s41398-019-0378-9.

(10) Ding, W.; Wu, F.; Zhou, S.; Li, H.; Wang, R.; Ning, Y. Increased Plasma Level of Kynurenic Acid in Drug-Free Patients with First-Episode Schizophrenia Compared to Patients with Chronic Schizophrenia and Healthy Controls: Preliminary Data. *https://doi.org/10.1080/08039488.2021.1992647* **2021**. https://doi.org/10.1080/08039488.2021.1992647.

(11) Huang, X.; Ding, W.; Wu, F.; Zhou, S.; Deng, S.; Ning, Y. Increased Plasma Kynurenic Acid Levels Are Associated with Impaired Attention/Vigilance and Social Cognition in Patients with Schizophrenia. *Neuropsychiatric Disease and Treatment* **2020**, *16*, 263. https://doi.org/10.2147/NDT.S239763.

(12) Chiappelli, J.; Pocivavsek, A.; Nugent, K. L.; Notarangelo, F. M.; Kochunov, P.; Rowland, L. M.; Schwarcz, R.; Hong, L. E. Stress-Induced Increase in Kynurenic Acid as a Potential Biomarker for Patients With Schizophrenia and Distress Intolerance. *JAMA Psychiatry* **2014**, *71* (7), 761–768. https://doi.org/10.1001/JAMAPSYCHIATRY.2014.243.

(13) Krause, D.; Myint, A. M.; Schuett, C.; Musil, R.; Dehning, S.; Cerovecki, A.; Riedel, M.; Arolt, V.; Schwarz, M. J.; Müller, N. High Kynurenine (a Tryptophan Metabolite) Predicts Remission in Patients with Major Depression to Add-on Treatment with Celecoxib. *Frontiers in Psychiatry* **2017**, *8* (FEB), 16. https://doi.org/10.3389/FPSYT.2017.00016/BIBTEX.

(14) Schwieler, L.; Samuelsson, M.; Frye, M. A.; Bhat, M.; Schuppe-Koistinen, I.; Jungholm, O.; Johansson, A. G.; Landén, M.; Sellgren, C. M.; Erhardt, S. Electroconvulsive Therapy Suppresses the Neurotoxic Branch of the Kynurenine Pathway in Treatment-Resistant Depressed Patients. *Journal of Neuroinflammation* **2016**, *13* (1), 1–10. https://doi.org/10.1186/S12974-016-0517-7/FIGURES/4.

(15) Zhou, Y.; Zheng, W.; Liu, W.; Wang, C.; Zhan, Y.; Li, H.; Chen, L.; Li, M.; Ning, Y. Antidepressant Effect of Repeated Ketamine Administration on Kynurenine Pathway Metabolites in Patients with Unipolar and Bipolar Depression. *Brain, Behavior, and Immunity* **2018**, *74*, 205–212. https://doi.org/10.1016/J.BBI.2018.09.007.

(16) Notarangelo, F. M.; Pocivavsek, A.; Schwarcz, R. Exercise Your Kynurenines to Fight Depression. *Trends in Neurosciences* **2018**, *41* (8), 491–493. https://doi.org/10.1016/J.TINS.2018.05.010.

(17) Erabi, H.; Okada, G.; Shibasaki, C.; Setoyama, D.; Kang, D.; Takamura, M.; Yoshino, A.; Fuchikami, M.; Kurata, A.; Kato, T. A.; Yamawaki, S.; Okamoto, Y. Kynurenic Acid Is a Potential Overlapped Biomarker between Diagnosis and Treatment Response for Depression from Metabolome Analysis. *Scientific Reports 2020 10:1* **2020**, *10* (1), 1–8. https://doi.org/10.1038/s41598-020-73918-z.

(18) Liu, H.; Ding, L.; Zhang, H.; Mellor, D.; Wu, H.; Zhao, D.; Wu, C.; Lin, Z.; Yuan, J.; Peng, D. The Metabolic Factor Kynurenic Acid of Kynurenine Pathway Predicts Major Depressive Disorder. *Frontiers in Psychiatry* **2018**, *9*, 552. https://doi.org/10.3389/FPSYT.2018.00552/BIBTEX.

(19) Atsumi, M.; Mawatari, K. I.; Morooka, A.; Yasuda, M.; Fukuuchi, T.; Yamaoka, N.; Kaneko, K.; Nakagomi, K.; Oku, N. Simultaneous Determination of Kynurenine and Kynurenic Acid by High-Performance Liquid Chromatography Photoirradiation System Using a Mobile Phase Containing 18-Crown-6. *International Journal of Tryptophan Research : IJTR* **2019**, *12*. https://doi.org/10.1177/1178646919834551.

(20) Perea, S.; Pennick, G. J.; Modak, A.; Fothergill, A. W.; Sutton, D. A.; Sheehan, D. J.; Rinaldi, M. G. Comparison of High-Performance Liquid Chromatographic and Microbiological Methods for Determination of Voriconazole Levels in Plasma. *Antimicrobial Agents and Chemotherapy* **2000**, *44* (5), 1209–1213. https://doi.org/10.1128/AAC.44.5.1209-1213.2000/ASSET/171D8A44-BF32-4B36-B5EA-8328291DB25B/ASSETS/GRAPHIC/AC0500648004.JPEG.

(21) Erabi, H.; Okada, G.; Shibasaki, C.; Setoyama, D.; Kang, D.; Takamura, M.; Yoshino, A.; Fuchikami, M.; Kurata, A.; Kato, T. A.; Yamawaki, S.; Okamoto, Y. Kynurenic Acid Is a Potential Overlapped Biomarker between Diagnosis and Treatment Response for

Depression from Metabolome Analysis. *Scientific Reports 2020 10:1* **2020**, *10* (1), 1–8. https://doi.org/10.1038/s41598-020-73918-z.

(22) Meier, T. B.; Drevets, W. C.; Teague, T. K.; Wurfel, B. E.; Mueller, S. C.; Bodurka, J.; Dantzer, R.; Savitz, J. Kynurenic Acid Is Reduced in Females and Oral Contraceptive Users: Implications for Depression. *Brain, Behavior, and Immunity* **2018**, *67*, 59–64. https://doi.org/10.1016/J.BBI.2017.08.024.

(23) Liu, H.; Ding, L.; Zhang, H.; Mellor, D.; Wu, H.; Zhao, D.; Wu, C.; Lin, Z.; Yuan, J.; Peng, D. The Metabolic Factor Kynurenic Acid of Kynurenine Pathway Predicts Major Depressive Disorder. *Frontiers in Psychiatry* **2018**, *9*, 552. https://doi.org/10.3389/FPSYT.2018.00552/BIBTEX.

(24) Liu, X. C.; Erhardt, S.; Goiny, M.; Engberg, G.; Mathé, A. A. Decreased Levels of Kynurenic Acid in Prefrontal Cortex in a Genetic Animal Model of Depression. *Acta Neuropsychiatrica* **2017**, *29* (1), 54–58. https://doi.org/10.1017/NEU.2016.31.

(25) Tanaka, M.; Bohár, Z.; Martos, D.; Telegdy, G.; Vécsei, L. Antidepressant-like Effects of Kynurenic Acid in a Modified Forced Swim Test. *Pharmacological Reports* **2020**, *72* (2), 449–455. https://doi.org/10.1007/S43440-020-00067-5/TABLES/1.

(26) Agudelo, L. Z.; Femenía, T.; Orhan, F.; Porsmyr-Palmertz, M.; Goiny, M.; Martinez-Redondo, V.; Correia, J. C.; Izadi, M.; Bhat, M.; Schuppe-Koistinen, I.; Pettersson, A. T.; Ferreira, D. M. S.; Krook, A.; Barres, R.; Zierath, J. R.; Erhardt, S.; Lindskog, M.; Ruas, J. L. Skeletal Muscle PGC-1α1 Modulates Kynurenine Metabolism and Mediates Resilience to Stress-Induced Depression. *Cell* **2014**, *159* (1), 33–45. https://doi.org/10.1016/J.CELL.2014.07.051.

(27) Schlittler, M.; Goiny, M.; Agudelo, L. Z.; Venckunas, T.; Brazaitis, M.; Skurvydas, A.; Kamandulis, S.; Ruas, J. L.; Erhardt, S.; Westerblad, H.; Andersson, D. C. Endurance Exercise Increases Skeletal Muscle Kynurenine Aminotransferases and Plasma Kynurenic Acid in Humans. *American Journal of Physiology - Cell Physiology* **2016**, *310* (10), C836–C840. https://doi.org/10.1152/AJPCELL.00053.2016/ASSET/IMAGES/LARGE/ZH001116793300003.JPEG.

(28) Lee, M. Y.; Lee, H. R.; Park, C. H.; Han, S. G.; Oh, J. H. Organic Transistor-Based Chemical Sensors for Wearable Bioelectronics. *Accounts of chemical research* **2018**, *51* (11), 2829–2838. https://doi.org/10.1021/ACS.ACCOUNTS.8B00465.

(29) Lee, Y. H.; Kweon, O. Y.; Kim, H.; Yoo, J. H.; Han, S. G.; Oh, J. H. Recent Advances in Organic Sensors for Health Self-Monitoring Systems. *Journal of Materials Chemistry C* **2018**, *6* (32), 8569–8612. https://doi.org/10.1039/C8TC02230E.

(30) Pinalli, R.; Pedrini, A.; Dalcanale, E. Biochemical Sensing with Macrocyclic Receptors. *Chemical Society Reviews* **2018**, *47* (18), 7006–7026. https://doi.org/10.1039/C8CS00271A.

(31) Sharma, A.; Khan, R.; Catanante, G.; Sherazi, T. A.; Bhand, S.; Hayat, A.; Marty, J. L. Designed Strategies for Fluorescence-Based Biosensors for the Detection of Mycotoxins. **2018**. https://doi.org/10.3390/toxins10050197.

(32) Katayev, E. A.; Ustynyuk, Y. A.; Sessler, J. L. Receptors for Tetrahedral Oxyanions. *Coordination Chemistry Reviews* **2006**, *250* (23–24), 3004–3037. https://doi.org/10.1016/J.CCR.2006.04.013.

(33) Karle, A.; Twum, K.; Sabbagh, N.; Haddad, A.; Taimoory, S. M.; Szczęśniak, M. M.; Trivedi, E.; Trant, J. F.; Beyeh, N. K. Naphthalene-Functionalized Resorcinarenes as

Potent and Highly- Selective, Fluorescent Self-Quenching, Sensors for Kynurenic Acid. *The Analyst, manuscript under review*, **2022**.
(34) Facts & Statistics | Anxiety and Depression Association of America, ADAA https://adaa.org/understanding-anxiety/facts-statistics (accessed 2022 -02 -14).
(35) Gallagher, M. W.; Zvolensky, M. J.; Long, L. J.; Rogers, A. H.; Garey, L. The Impact of Covid-19 Experiences and Associated Stress on Anxiety, Depression, and Functional Impairment in American Adults. *Cognitive Therapy and Research* **2020**, *44* (6), 1043–1051. https://doi.org/10.1007/S10608-020-10143-Y/TABLES/4.
(36) Mousa, O. Y.; Dhamoon, M. S.; Lander, S.; Dhamoon, A. S. The MD Blues: Under-Recognized Depression and Anxiety in Medical Trainees. *PLOS ONE* **2016**, *11* (6), e0156554. https://doi.org/10.1371/JOURNAL.PONE.0156554.
(37) Hutchens, B. F.; Kearney, J. Risk Factors for Postpartum Depression: An Umbrella Review. *Journal of Midwifery & Women's Health* **2020**, *65* (1), 96–108. https://doi.org/10.1111/JMWH.13067.
(38) Bauman, B. L.; Ko, J. Y.; Cox, S.; D'Angelo, MPH, D. v.; Warner, L.; Folger, S.; Tevendale, H. D.; Coy, K. C.; Harrison, L.; Barfield, W. D. Vital Signs: Postpartum Depressive Symptoms and Provider Discussions About Perinatal Depression — United States, 2018. *MMWR. Morbidity and Mortality Weekly Report* **2020**, *69* (19), 575–581. https://doi.org/10.15585/MMWR.MM6919A2.
(39) Ross, R. A.; Kaiser, U. B. The Emotional Cost of Contraception. *Nature reviews. Endocrinology* **2016**, *13* (1), 7. https://doi.org/10.1038/NRENDO.2016.194.
(40) Wurfel, B. E.; Drevets, W. C.; Bliss, S. A.; McMillin, J. R.; Suzuki, H.; Ford, B. N.; Morris, H. M.; Teague, T. K.; Dantzer, R.; Savitz, J. B. Serum Kynurenic Acid Is Reduced in Affective Psychosis. *Translational psychiatry* **2017**, *7* (5). https://doi.org/10.1038/TP.2017.88.
(41) Erabi, H.; Okada, G.; Shibasaki, C.; Setoyama, D.; Kang, D.; Takamura, M.; Yoshino, A.; Fuchikami, M.; Kurata, A.; Kato, T. A.; Yamawaki, S.; Okamoto, Y. Kynurenic Acid Is a Potential Overlapped Biomarker between Diagnosis and Treatment Response for Depression from Metabolome Analysis. *Scientific Reports 2020 10:1* **2020**, *10* (1), 1–8. https://doi.org/10.1038/s41598-020-73918-z.
(42) Tanaka, M.; Bohár, Z.; Martos, D.; Telegdy, G.; Vécsei, L. Antidepressant-like Effects of Kynurenic Acid in a Modified Forced Swim Test. *Pharmacological Reports* **2020**, *72* (2), 449–455. https://doi.org/10.1007/S43440-020-00067-5/TABLES/1.
(43) Liu, H.; Ding, L.; Zhang, H.; Mellor, D.; Wu, H.; Zhao, D.; Wu, C.; Lin, Z.; Yuan, J.; Peng, D. The Metabolic Factor Kynurenic Acid of Kynurenine Pathway Predicts Major Depressive Disorder. *Frontiers in Psychiatry* **2018**, *9*, 552. https://doi.org/10.3389/FPSYT.2018.00552/BIBTEX.
(44) Savitz, J. Role of Kynurenine Metabolism Pathway Activation in Major Depressive Disorders. *Current topics in behavioral neurosciences* **2017**, *31*, 249–268. https://doi.org/10.1007/7854_2016_12.
(45) Baratta, A. M.; Viechweg, S. S.; Mong, J. A.; Pocivavsek, A. A High-Performance Liquid Chromatography Measurement of Kynurenine and Kynurenic Acid: Relating Biochemistry to Cognition and Sleep in Rats. *Journal of Visualized Experiments : JoVE* **2018**, *2018* (138), 58129. https://doi.org/10.3791/58129.
(46) Azeotropic Distillation with Interesting Examples and Applications https://www.studyread.com/azeotropic-distillation-examples/ (accessed 2022 -02 -07).

(47) Rotary Evaporation: The “Rotovap” http://www.chem.ucalgary.ca/courses/351/laboratory/rotavap.pdf.
(48) Scheller, F. W.; Wollenberger, U.; Warsinke, A.; Lisdat, F. Research and Development in Biosensors. *Current Opinion in Biotechnology* **2001**, *12* (1), 35–40. https://doi.org/10.1016/S0958-1669(00)00169-5.
(49) Turski, M. P.; Turska, M.; Paluszkiewicz, P.; Parada-Turska, J.; Oxenkrug, G. F. Kynurenic Acid in the Digestive System—New Facts, New Challenges. *International Journal of Tryptophan Research : IJTR* **2013**, *6* (6), 47. https://doi.org/10.4137/IJTR.S12536.
(50) Hsu, C. N.; Tain, Y. L. Developmental Programming and Reprogramming of Hypertension and Kidney Disease: Impact of Tryptophan Metabolism. *International Journal of Molecular Sciences 2020, Vol. 21, Page 8705* **2020**, *21* (22), 8705. https://doi.org/10.3390/IJMS21228705.
(51) Owens, P. L.; Fingar, K. R.; McDermott, K. W.; Muhuri, P. K.; Heslin, K. C. Inpatient Stays Involving Mental and Substance Use Disorders, 2016: Statistical Brief #249. *Healthcare Cost and Utilization Project (HCUP) Statistical Briefs* **2019**.